Experimental determination of the internal quantum efficiency of AlGaInP microcavity light-emitting diodes

P. Royo,[a] R. P. Stanley, and M. Ilegems
Institut de Micro et Opto-Electronique, Ecole Polytechniqúe Fédérale de Lausanne, CH-1015 Lausanne EPFL, Switzerland

K. Streubel[b]
Mitel Semiconductor AB, Bruttovägen 1, Box 520, S-17526 Järfälla, Sweden

K. H. Gulden
Avalon Photonics Ltd, Badenerstrasse 569, CH-8048 Zürich, Switzerland

(Received 21 September 2001; accepted for publication 16 November 2001)

Detailed study of external quantum efficiency η_{QE} is reported for AlGaInP-based microcavity light-emitting diodes (MCLEDs). Unlike conventional light-emitting diodes (LEDs) the extraction efficiency γ_{ext} and far field profile depend on the linewidth of the intrinsic spontaneous emission and wavelength detuning between cavity mode and peak electroluminescence. This dependence makes it difficult to estimate the intrinsic spectrum, hence the performances of MCLEDs. By using a nondestructive deconvolution technique, the intrinsic spectra of a MCLED and a reference LED (with the same active regions) could be determined at different current densities. This allowed precise calculation of γ_{ext} for both devices (values close to 11% were found for the MCLED), and hence of their apparent internal quantum efficiencies η_{int}^{app}. At 55 A/cm^2, values of 90% and 40% were determined for the LED and MCLED, respectively. In order to explain this difference, we measured η_{QE} for devices with different sizes. From a fitting procedure based on a simple model taking into account the device size, we found that the radiative efficiencies of LEDs and MCLEDs were close to 90%. We concluded that the low η_{int}^{app} of MCLED was due to a bad current injection, and especially to electron leakage current, as confirmed by numerical simulations. © *2002 American Institute of Physics.* [DOI: 10.1063/1.1433938]

I. INTRODUCTION

Because of their high brightness, narrow linewidth, and high extraction efficiency per facet, microcavity light-emitting diodes (MCLEDs) are of great interest for low-cost applications like optical fiber networks or short distance optical interconnects.[1–4] MCLED structures consist of an active medium placed at the antinode of a low order cavity surrounded by two mirrors which can be either metallic or dielectric.

An important figure of merit of these devices is the external quantum efficiency, which is defined as the ratio between the flux of emitted photons and the flux of injected electrons $\eta_{QE}=\Phi_{ext}/\Phi_{el}$. Because of total internal reflection, most of the light generated in the semiconductor cannot be directly extracted. The ratio between the flux of emitted photons and the flux of photons generated inside the semiconductor is defined as the extraction efficiency $\gamma_{ext}=\Phi_{ext}/\Phi_{int}$. Simple calculations[5] show that for single facet planar nonmicrocavity devices $\gamma_{ext}=0.5(1-\cos\theta_c)$ for isotropic emission in the semiconductor. The critical angle $\theta_c=\arcsin(n_{out}/n_{sc})$ depends on the refractive indices of the outside medium (n_{out}) and semiconductor (n_{sc}). For most of the III/V semiconductors, extraction efficiencies (per facet) close to 2% (4%) in air (epoxy) are found. On the contrary, for MCLEDs, γ_{ext} depends strongly on the combined properties of the passive cavity and of the intrinsic spectrum $r_{spont}(\lambda)$ emitted by the active region inside the device.[6,7] These last few years, a much effort has been devoted to optimizing and studying the extraction efficiency of MCLEDs.[7–11] Hence, as the extraction efficiency of LEDs significantly increases, there is more interest and need in optimizing the electron to photon conversion efficiency of these devices, i.e., the internal quantum efficiency $\eta_{int}=\Phi_{int}/\Phi_{el}$. Although this parameter can be easily measured at high current densities for lasers,[12] no simple way of determining η_{int} exists for LEDs operating at low current densities. The simplest method is to measure η_{QE} and to calculate γ_{ext}, which allows calculation of $\eta_{int}=\eta_{QE}/\gamma_{ext}$. The accuracy of this procedure relies on the calculation of γ_{ext}, which is difficult to determine precisely for nonplanar LEDs. In contrast, numerical methods for simulations of planar multilayer emitters are readily available.[13] For MCLEDs, the main difficulty for accurate calculation of the extraction efficiency is to determine precisely the intrinsic spectrum $r_{spont}(\lambda)$ emitted by the active region. Indeed, because the spontaneous emission is generated between two close and highly reflective mirrors, the emitted light is coupled to the optical modes of the cavity which dominates the externally

[a]Present address: Department of Electrical and Computer Engineering, University of California, Santa Barbara, CA 93106; electronic mail: royo@ece.ucsb.edu
[b]Present address: Osram Opto Semiconductors, Wernerwerkstrasse 2, D-93049 Regensburg, Germany.

observed spectrum. The simplest method to estimate $r_{spont}(\lambda)$ relies then on destructive techniques. The most common methods are to measure the photoluminescence from either a cleaved edge of the wafer or from the active region after etching off the top mirror. We recently showed[14,15] that using angle-resolved measurements of the top-emission spectra and comparison with numerical simulations, it was possible to precisely and nondestructively measure $r_{spont}(\lambda)$.

The first objective of this article is to apply this technique to AlGaInP-based MCLEDs emitting at 650 nm. Light sources emitting at this wavelength are indeed of great interest for local area networks based on plastic optical fibers which exhibit a minimum of absorption at this wavelength.[3] It is well known that red AlGaInP-based MCLEDs and VCSELs suffer from bad injection efficiency compared to infrared AlGaAs-based emitters because of less favorable material properties such as smaller carrier confinement potential and larger effective masses.[19,20] It is then of great interest to determine the internal quantum efficiency of these devices so as to optimize the design of their active region. The first section of this article describes the design and the fabrication of the devices investigated. The second section presents the determination of the internal quantum efficiency of an AlGaInP-based MCLEDs and of planar nonresonant cavity LED which was grown for comparison purposes. We show that η_{int} is 2.25 times higher for the nonresonant cavity LED compared to the MCLED.

The second part of this article is then devoted to explaining this difference. For that purpose, the current density dependence of the external quantum efficiency η_{QE} is approximated by a simple analytical expression which involves the lateral size of the devices. Measurement of η_{QE} for both kinds of devices and for different lateral sizes allowed us to explain why η_{int} is higher for the nonresonant cavity LED than for the MCLED.

II. DESCRIPTION OF THE DEVICES AND PROCESSING

The MCLED structure studied here is the same as the one presented in Ref. 3. It consists of GaInP quantum wells surrounded by AlGaInP spacer layers forming a one-lambda cavity. The two distributed Bragg reflectors (DBRs) surrounding the active region consist of alternating layers of AlGaAs and AlAs materials. These devices are processed into planar top-emitting devices: square shape mesa are dry etched through the active region so as to define current confining structures. The width of the mesas is 262 μm. Plasma enhanced chemical vapor deposition of Si_3N_4 is used for passivation of the wafer surface and for electrical isolation of adjacent diodes. Windows are then dry etched in the Si_3N_4 covering top of the mesa. Top contacts are deposited on the mesa by lift-off technique. The current is injected in the mesa through a grid with honeycomb geometry (masking part of the mesa's surface) so as to spread the current uniformly over the active region. Because of the large surface of the device, this grid is required to prevent current crowding. The bottom contacts are evaporated on the whole surface of the substrate. The processed devices are finally bonded and mounted on TO-46 headers. The fabrication of these devices ensures that light is emitted through the top facet of the wafer only. Figure 1 shows the optical microscope picture of a processed MCLED (a), and its cross section (b). For comparison purposes, a reference LED structure was grown with the DBRs replaced by AlGaInP cladding layers surrounding the same active region as the MCLED.

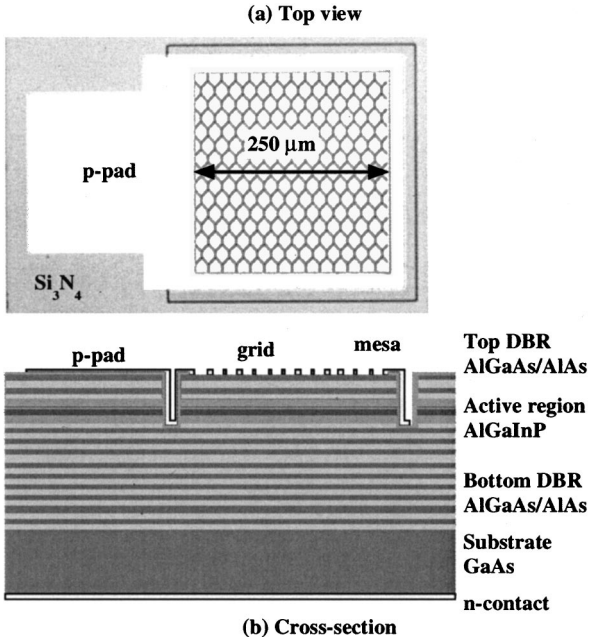

FIG. 1. (a) Optical microscope picture of a processed device. (b) Cross section of the MCLED (not on scale).

III. DETERMINATION OF THE EXTRACTION EFFICIENCY

For large size MCLEDs, γ_{ext} can be numerically determined by using the model described in Ref. 13. The spontaneous emission is calculated in the dipole approximation by using a plane and evanescent wave decomposition of the radiation. Propagation of these waves inside the MCLED is calculated with the transfer matrix formalism. The extraction efficiency of the MCLED γ_{ext} can then be calculated provided the intrinsic spontaneous emission spectrum $r_{spont}(\lambda)$ of the quantum wells is known. Indeed, contrary to conventional LEDs for which γ_{ext} depends mainly on the device geometry, the extraction efficiency of MCLEDs depends critically on the combined properties of the cavity and intrinsic spectrum.[6,7] Precise calculation of the MCLED's extraction efficiency requires accurate knowledge of the passive MCLED's structure (indices of refraction and thicknesses of the layers), and of $r_{spont}(\lambda)$ at the chosen current density. Indeed, the intrinsic spectrum is the product between the joint density of states of the active region, their occupation probability, and a function describing line shape broadening effects.[12] Hence the intrinsic spectrum $r_{spont}(\lambda)$ greatly depends on the injected current density.

In order to calculate the MCLED extraction efficiency, the first step is to accurately determine the layer thicknesses. Using the model described in Ref. 13, the angle-resolved

top-emission spectra $\Pi_{ext}(\theta,\lambda)$ of any planar multilayer structure emitting in the spontaneous regime can be expressed as

$$\Pi_{ext}(\theta,\lambda)=r_{spont}(\lambda)\Pi_{sim}(\theta,\lambda), \quad (1)$$

where $\Pi_{sim}(\theta,\lambda)$ is the response of the optical system to a white spectral source and θ the angle defined with respect to the growth axis. This relation allows us to iteratively determine the actual structure of the MCLED: starting from the nominal layer thicknesses, the angular dependence of $\Pi_{sim}(\theta,\lambda)$ can be numerically calculated at each wavelength λ and compared to those of $\Pi_{ext}(\theta,\lambda)$, which is determined by angle-resolved spectral measurements. Since the intrinsic spectrum does not depend on the angle θ, this procedure can be performed at any chosen current density. Because of the microcavity, $\Pi_{ext}(\theta,\lambda)$ and $\Pi_{sim}(\theta,\lambda)$ display very sharp resonances that are easy to match by iteratively adjusting the layer thicknesses of the DBRs and of the cavity. This works when the nominal and actual thicknesses are not too different.

The second step of the γ_{ext} determination consists of measuring $r_{spont}(\lambda)$. For our MCLEDs, the active medium is at the antinode of a low-order cavity defined by the two DBRs. Consequently, the intrinsic spectrum emitted by the active region is coupled to the cavity modes, which completely dominate the externally observed spectrum $\Pi_{ext}(\theta,\lambda)$, and is then difficult to measure directly without destruction of the device. Indeed, the most common methods consist of measuring $r_{spont}(\lambda)$ from either a cleaved wafer edge or from the active region after etching off the top mirror. The method chosen in this work relies on a deconvolution procedure presented in Refs. 14 and 15, which is nondestructive and takes advantage of the angle-resolved spectral measurements. The intrinsic spectra were determined by the deconvolution procedure for ten current densities between 15 and 145 A/cm^2. The device were driven in quasicontinuous mode: voltage pulses of 500 μs were applied at a frequency of 1 kHz. We observed that for these rather small current densities, the deconvolved intrinsic spectra are well fitted by the following function:

$$r_{spont}(\lambda)=\frac{2e^{[cm(\lambda-\lambda_{QW})]}}{2-c+ce^{[2m(\lambda-\lambda_{QW})]}}, \quad (2)$$

where λ_{QW} is the peak electroluminescence of the quantum wells and *c*, *m* some fitting constants. This function presents two exponential tails for wavelengths far from λ_{QW} with different slopes and displays a maximum at $\lambda=\lambda_{QW}$. The parameter *c* describes the asymmetry of the function whereas *m* is related to its full width at half maximum (FWHM). The physical justification of this empirical function, based on a super-radiance model, is given in Ref. 16. Figure 2 displays the spontaneous spectrum measured on a reference LED (which has nominally the same active region as the MCLED) at a current density of 36 A/cm^2.

Fitting the deconvolved spectra with function (2) then allowed us to characterize $r_{spont}(\lambda)$ by the wavelength of emission λ_{QW}, and the FWHM σ_{QW}, which is mainly related to the coefficient *m* (*c* was found to be constant and close to 1.5 for the considered current densities). The extraction efficiency of the MCLED was then calculated numerically for different couples (λ_{QW}, σ_{QW}) using the thicknesses which were previously determined. Result of these calculations are shown in Fig. 3: the contour lines of γ_{ext} are displayed as solid lines for extraction efficiencies between 7% and 17%. The horizontal axis represents the quantum well emission wavelength λ_{QW} and the vertical one the source linewidth σ_{QW}. The vertical dotted line represents the position of the Fabry–Pérot resonance λ_{FP} determined by the cavity and DBR layers thicknesses. The difference between

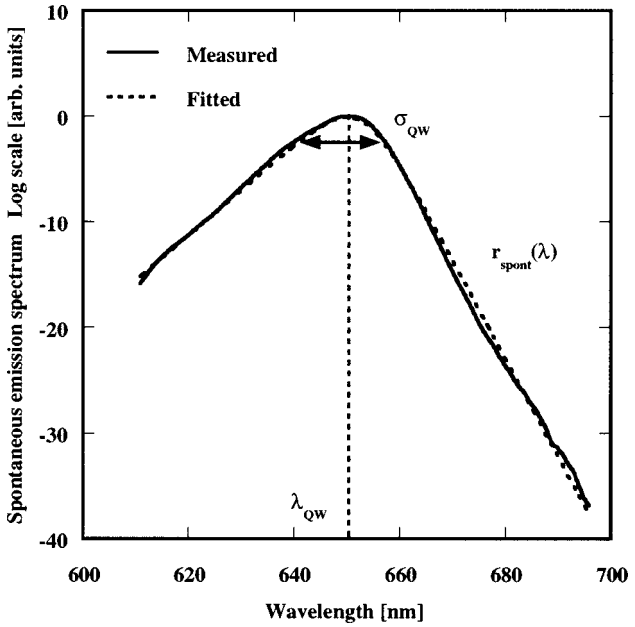

FIG. 2. Electroluminescence spectrum measured at normal incidence (solid line) for the reference LED, at a current density of 36 A/cm^2. The dotted line represents a fit using the analytical expression of $r_{spont}(\lambda)$.

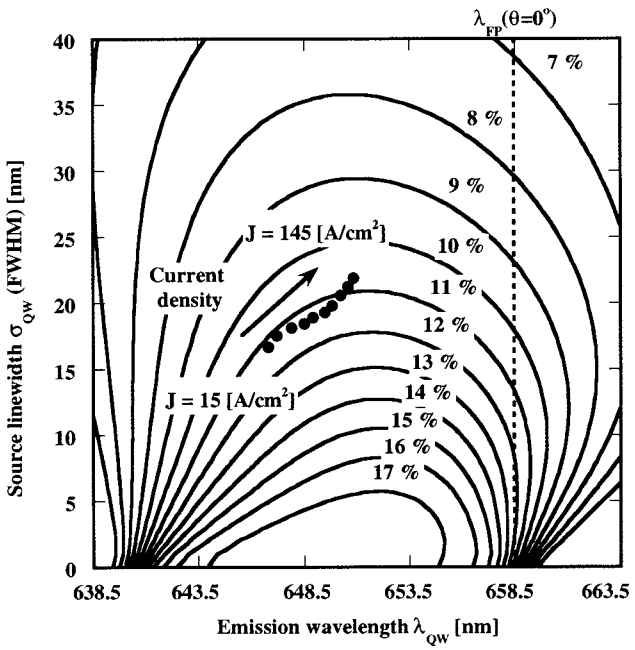

FIG. 3. Contour plot of the extraction efficiency calculated for different values of quantum well emission wavelengths and linewidths. Closed circles represent experimental values measured between 15 and 145 A/cm^2.

λ_{QW} and λ_{FP} is often defined as the cavity-source detuning: $\Delta\lambda = \lambda_{QW} - \lambda_{FP}$. The extraction efficiency is maximum for negative detunings whatever the source linewidth σ_{QW} is and the linewidth broadening always decreases γ_{ext}. Because of the microcavity, light emitted by the active region is redirected into the Fabry–Pérot modes which are extracted provided they fit in the cone of half-angle θ_c (also called the escape cone). When the detuning is zero, the intrinsic spectrum is in resonance with the cavity mode at normal incidence. When the detuning is negative, the resonance between the intrinsic emission and the cavity is found at a larger angle, and the maximum light output occurs at this angle. This increases the extraction efficiency.[6,7]

Figure 3 displays as closed circles the extraction efficiencies calculated for the parameters $(\lambda_{QW}, \sigma_{QW})$ measured with the deconvolution technique, at different current densities. The measured γ_{ext} follow approximately the 11% contour line of Fig. 3. Here, the effect of spectral broadening (which always decreases γ_{ext}) is compensated by redshift of the spontaneous emission (mainly due to heating): measured γ_{ext} then remains on a contour line of Fig. 3. In contrast, one sees that if the detuning was close to zero at low current density, then the extraction efficiency would tend to follow the gradient of the contour line with increasing current density, implying a significant decrease of γ_{ext}. We should point out that it is easier to calculate the γ_{ext} of a MCLED than a LED. The multilayers of MCLEDs are indeed easier to distinguish in reflectivity. The γ_{ext} of MCLEDs is not that sensitive to layer thickness changes and mainly depends on the intrinsic spectrum properties, which can be accurately determined by the deconvolution technique, and which can be confirmed with LED measurements. In LEDs, there are also incoherent reflections and scattering very difficult to parametrize, whereas MCLEDs are only coherent.

IV. DETERMINATION OF THE INTERNAL QUANTUM EFFICIENCY

The extraction efficiency being known, we can determine the apparent internal quantum efficiency after measuring the external quantum efficiency: $\eta_{int}^{app} = \eta_{QE}/\gamma_{ext}$. The optical power emitted by the MCLED was measured by using an integrating sphere so as to collect all the emitted light. Figure 4 displays the voltage (left axis) and optical power (right axis) versus the injected current for the LED (dotted line) and MCLED (solid line). The corresponding external quantum efficiencies were found to peak to 4.5% (1.75%) at 55 A/cm^2 (50 A/cm^2) for the MCLED (LED). Figure 5 displays the apparent internal quantum efficiency calculated for LED and MCLED as a function of the injected current density. A maximum of 40% (90%) is found at 55 A/cm^2 (60 A/cm^2) for the MCLED (LED). While the internal quantum efficiency reported for this MCLED is consistent with other AlGaInP-based MCLEDs,[17,18] its value is significantly lower than in conventional LEDs. Considering the semiconductor rate equation, the apparent internal quantum efficiency of LEDs and MCLEDs can be approximately expressed as the product between a shadowing efficiency η_{sh} (representing the effect of grid shadowing and current crowding effects on

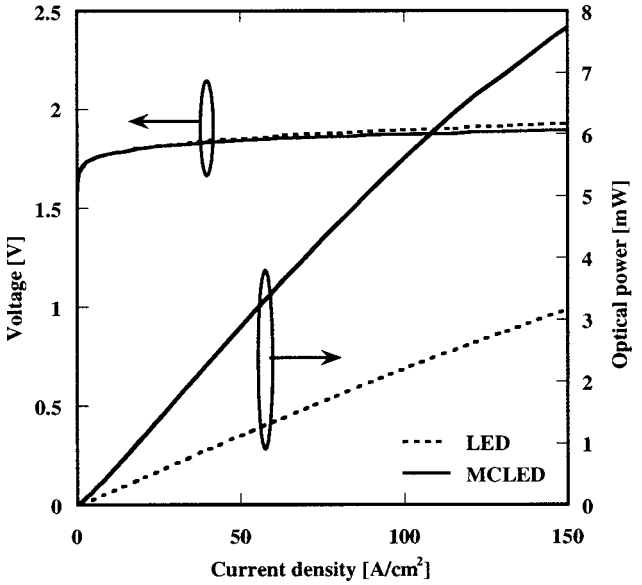

FIG. 4. Voltage–current density characteristics (left axis) and power–current density characteristics (right axis) for the LED (dotted line) and MCLED (solid line).

light emission), a radiative efficiency η_r (defined as the ratio between radiative recombinations and total recombinations in the active region), and an injection efficiency η_i (representing the fraction of terminal current that generates carriers in the active region).[12] Table I lists the different definitions of the efficiencies used in this work. Since the processing and the geometries of both devices are the same, the significant difference observed on their apparent quantum efficiency is due to either a poor radiative efficiency or a poor injection efficiency of the MCLED. We indeed checked by near-field experiments and by differential and sheet resistance mea-

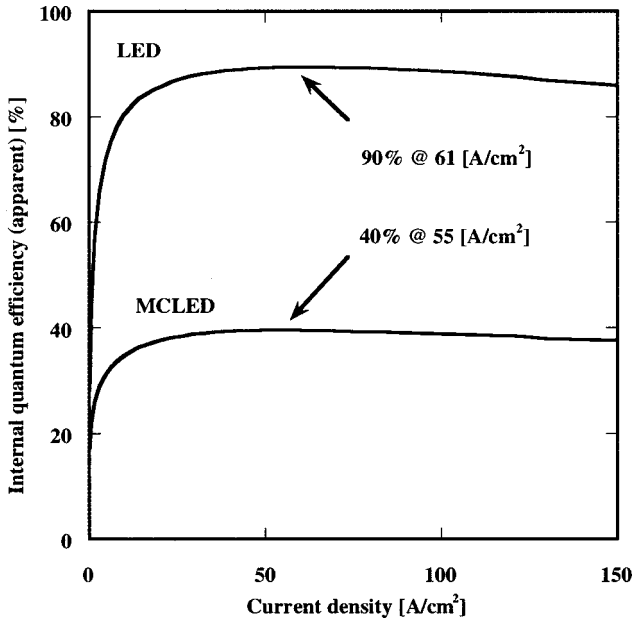

FIG. 5. Apparent internal quantum efficiency of the LED and MCLED plotted vs the current density.

TABLE I. Definitions of the efficiencies used in this work.

Parameter	Definition
$\eta_{QE}=\gamma_{ext}\eta_{int}^{app}$	External quantum efficiency
γ_{ext}	Extraction efficiency
$\eta_{int}^{app}=\eta_{sh}\eta_r\eta_i$	Internal quantum efficiency (apparent)
η_{sh}	Shadowing efficiency
η_r	Radiative efficiency
η_i	Injection efficiency

surements, that at these low current densities, current crowding underneath the grid was of the same order of magnitude for both devices and could be neglected.

V. STUDY OF THE EXTERNAL QUANTUM EFFICIENCY

Let us first consider the radiative efficiency η_r. This parameter is the ratio between the radiative recombination rate and total recombination rate in the active region, which can be expressed with respect to the carrier density in the active region N by $\eta_r=BN^2/(AN+BN^2)$. The coefficient B is the bimolecular recombination coefficient, and the nonradiative recombination rate can be expressed as AN with $A=A_0+4v_s/\sqrt{S_{mesa}}$. The term A_0 is the inverse of a capture rate describing nonradiative recombinations related to bulk defects and impurities, whereas v_s is a recombination rate velocity describing surface and interface nonradiative recombination mechanisms.[12] The surface of the active region is S_{mesa} and its total thickness is L_a. Auger nonradiative recombinations can be neglected: for high band gap alloys like AlGaInP, this effect is small because the split off valence band gap ($\Delta_0=0.1$ eV) is much smaller than the direct band gap energy ($E_\Gamma=2$ eV), resulting in small Auger coefficients.[19] Using the continuity equation $(\eta_i J)/(eL_a)=AN+BN^2$ (e is the electron charge), one finds the following current dependence ($I=JS_{mesa}$) of the radiative efficiency:

$$\eta_r(I)=\frac{I_0}{I}\left[1+\frac{I}{I_0}-\sqrt{1+\frac{I}{I_0}}\right], \tag{3}$$

where I_0 is a characteristic current defined as

$$I_0=\frac{e}{2}\frac{L_a}{\eta_i}\frac{A_0^2}{B}S_{mesa}\left[1+\frac{4v_s}{A_0\sqrt{S_{mesa}}}\right]^2. \tag{4}$$

Relation (3) is derived assuming that the injection efficiency does not vary rapidly with the current. The radiative efficiency calculated with Eq. (3) continuously increases with the current and saturates to one (when the carrier density is large enough, the radiative recombination rate dominates the nonradiative recombination rate). Note that the smaller the characteristic current I_0, the quicker $\eta_r(I)$ converges to one. For the MCLEDs and LEDs we are considering, the efficiencies γ_{ext}, η_i, and η_{sh} decrease as the current density increases. Since these factors contribute to the rollover of the devices, we use the following phenomenological function to describe their combined current dependence:

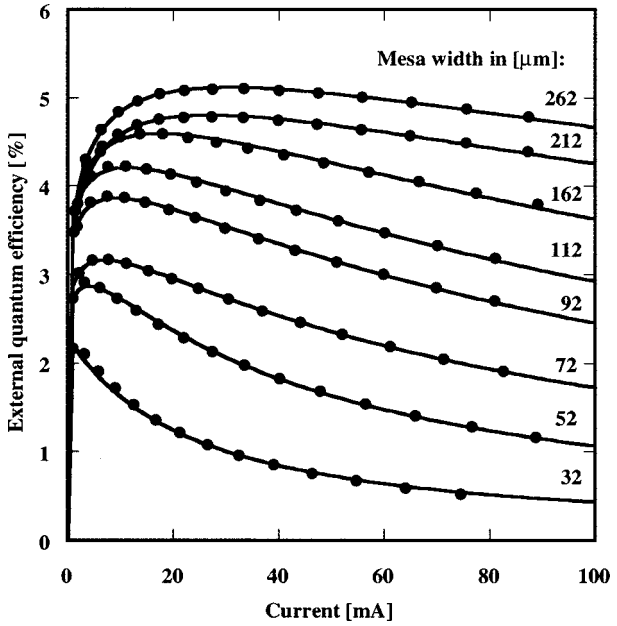

FIG. 6. External quantum efficiencies measured on MCLEDs with various mesa widths (closed circles). The solid lines represent the external quantum efficiencies fitted from the simple model.

$$\eta_0(I)=\eta_{sh}(I)\,\eta_i(I)\,\gamma_{ext}(I)=\frac{\eta_s}{1+\dfrac{I}{I_s}}, \tag{5}$$

where η_s and I_s are two constants. The efficiency $\eta_0(I)$ is close to η_s at very small current, and decreases with the current. Note that the higher I_s is, the slower this function decreases. The external quantum efficiency can then be approximated by the following relation: $\eta_{QE}(I)=\eta_r(I)\,\eta_0(I)$.

The characteristic current I_0 depends on the surface of the mesa. Hence, fitting the measured $\eta_{QE}(I)$ with expressions (3) and (5) for different device sizes, we can deduce the surface dependence of $I_0=I_0(S_{mesa})$, from which the physical parameters $A_0^2/(B\eta_i)$ and v_s/A_0 can be deduced. Figure 6 displays as closed circles the external quantum efficiencies measured on MCLEDs with various mesa widths $D=\sqrt{S_{mesa}}$ as function of the injected current. The solid lines represent the external quantum efficiencies fitted from the simple model. Considering the simplicity of the model and the small number of fitting constants (η_s, I_s and I_0), the agreement between measurements and calculations is good. Measurement of the external quantum efficiency was performed on LEDs with the same mesa widths. The analytical expression of $\eta_{QE}(I)$ was also found to agree well with measurements. The characteristic currents I_0 were extracted for both types of devices and are plotted as closed (open) circles in Fig. 7 with respect to the surface of the mesa S_{mesa} for the MCLED (LED). These values were then fitted using the expression $I_0=I_0(S_{mesa})$ given in Eq. (4). Results are shown as solid (dotted) lines for the MCLED (LED). The good agreement between measured and calculated $I_0=I_0(S_{mesa})$ indicates the consistency of the simplified model presented here. These results show that at low current, $\eta_{QE}(I)$ is dominated by the radiative efficiency factor $\eta_r(I)$, which can be reasonably approximated by expression (3). From the fits

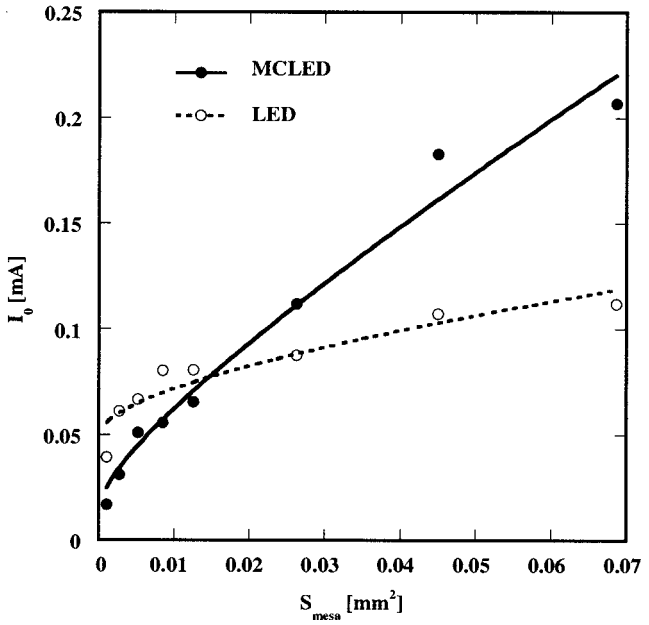

FIG. 7. Characteristic current plotted vs the surface of the mesa. Closed (open) circles represent values extracted from the fits on the measured for the MCLED (LED). Solid (dotted) lines correspond to analytical expressions.

performed on the data displayed in Fig. 7 we get: $(eL_aA_0^2)/(2B\eta_i)=22\ \mathrm{mA/cm^2}$ for LEDs and $(eL_aA_0^2)/(2B\eta_i)=184\ \mathrm{mA/cm^2}$ for MCLEDs. The ratio $4v_s/A_0$ is equal to 470 μm for LEDs and 84 μm for MCLEDs. It is difficult to obtain reasonable values of A_0, v_s, and B from these results because our simple model provides ratios of these coefficients only. However, we can use the extracted values of $(eL_aA_0^2)/(2B\eta_i)$ and $4v_s/A_0$ so as to determine the radiative efficiency of the large size diodes for which we determined the apparent internal quantum efficiency in Sec. IV. We find that, for $D=262$ μm and at 55 $\mathrm{A/cm^2}$, the radiative efficiency of the LED and MCLED is approximately the same ($\eta_r=0.95$ and $\eta_r=0.92$). Figure 5 shows that at this current density, the apparent internal quantum efficiency of the LED is 2.25 times higher than for the MCLED. We conclude that at this current density, the injection efficiency of the MCLED is about two times smaller than for the LED. Preliminary investigations indicate that the injection problem arises in MCLEDs due to the limitations of the AlGaAs-based mirror surrounding the thin (one-lambda) AlGaInP-based active region, and due to electron confinement, which is a well-known obstacle for red VCSELs.[19–21]

VI. CONCLUSION

In conclusion, the external quantum efficiency of AlGaInP-based MCLEDs was measured. By using a nondestructive deconvolution technique, the intrinsic spectra of a MCLED and a reference LED (with the same active regions) could be determined at different current densities. This allowed precise calculation of the extraction efficiency for both devices (values close to 11% were found for the MCLED), hence of their apparent internal quantum efficiencies. At 55 $\mathrm{A/cm^2}$, values of 90% and 40% were determined for the LED and MCLED, respectively. In order to explain this difference, we measured the external quantum efficiencies of LEDs and MCLEDs with different sizes. From a fitting procedure based on a simple model taking into account the device size, it was found that the radiative efficiencies of the large size LEDs and MCLEDs were close to 90%. It was concluded that the low apparent internal quantum efficiency measured on the MCLED was due to a bad current injection, and especially to electron leakage current. It is demonstrated that it is possible to accurately determine the extraction efficiency and the internal quantum efficiency of MCLEDs. This procedure can then be applied to optimize the design of their active region and their injection efficiency.

ACKNOWLEDGMENT

This work was supported by the European Commission within the framework of the ESPRIT-SMILED program.

[1] E. F. Schubert, Y. H. Wang, A. Y. Cho, L. W. Tu, and G. J. Zydzik, Appl. Phys. Lett. **60**, 921 (1992).
[2] J. A. Lott, R. P. Schneider, G. A. Vawter, J. C. Zolper, and K. J. Malloy, IEEE Photonics Technol. Lett. **5**, 631 (1993).
[3] K. Streubel, U. Helin, V. Oskarsson, E. Bäcklin, and Å. Johansson, IEEE Photonics Technol. Lett. **10**, 1685 (1998).
[4] R. Bockstaele, C. Sys, J. Blondelle, B. Dhoedt, I. Moermann, P. Van Daele, P. Demeester, and R. Baets, IEEE Photonics Technol. Lett. **11**, 158 (1999).
[5] M. G. Craford and G. B. Stringfellow, *High Brightness Light Emitting Diodes, Semiconductors and Semimetals* (Academic, San Diego, 1997), Vol. 48.
[6] H. Benisty, H. De Neve, and C. Weisbuch, IEEE J. Quantum Electron. **34**, 1612 (1998).
[7] P. Royo, R. P. Stanley, and M. Ilegems, J. Appl. Phys. **90**, 283 (2001).
[8] N. E. Hunt, E. F. Schubert, R. F. Kopf, D. L. Sivco, A. Y. Cho, and G. J. Zydzik, Appl. Phys. Lett. **63**, 2600 (1993).
[9] J. Blondelle, H. De Neve, P. Demeester, P. Van Daele, G. Borghs, and R. Baets, Electron. Lett. **31**, 1286 (1995).
[10] H. De Neve, J. Blondelle, R. Baets, P. Demeester, P. Van Daele, and G. Borghs, IEEE Photonics Technol. Lett. **7**, 287 (1995).
[11] C. Dill, R. P. Stanley, U. Oesterle, D. Ochoa, and M. Ilegems, Appl. Phys. Lett. **73**, 3812 (1998).
[12] L. A. Coldren and S. Corzine, *Diode Lasers and Photonic Integrated Circuits* (Wiley, New York, 1995).
[13] H. Benisty, M. Mayer, and R. P. Stanley, J. Opt. Soc. Am. A **15**, 1192 (1998).
[14] P. Royo, R. P. Stanley, M. Ilegems, K. Streubel, and K. H. Gulden, Appl. Phys. Lett. **77**, 3899 (2000).
[15] P. Royo, R. P. Stanley, M. Ilegems, K. H. Gulden, and K. Streubel, Electron. Lett. **36**, 2106 (2000).
[16] S. V. Zaitsev, N. Yu. Gordeev, L. Ya. Karachinsky, V. I. Kopchatov, I. I. Novikov, I. S. Tarasov, N. A. Pikhtin, V. M. Ustinov, and P. S. Kop'ev, Appl. Phys. Lett. **76**, 2514 (2000).
[17] P. Royo, R. P. Stanley, R. Houdré, M. Ilegems, M. Moser, R. Hövel, H. P. Schweizer, and K. H. Gulden, Appl. Phys. Lett. **75**, 4052 (1999).
[18] M. Jalonen, J. Köngäs, M. Toivonen, P. Savolainen, A. Salokatve, and M. Pessa, IEEE Photonics Technol. Lett. **10**, 923 (1998).
[19] D. P. Bour, D. W. Treat, R. L. Thornton, R. S. Geels, and D. F. Welch, IEEE J. Quantum Electron. **29**, 1337 (1993).
[20] P. M. Smowton and P. Blood, IEEE J. Sel. Top. Quantum Electron. **3**, 491 (1997).
[21] W. W. Chow, K. D. Choquette, M. H. Crawford, K. L. Lear, and G. R. Hadley, IEEE J. Quantum Electron. **33**, 1810 (1997).